

## Crystal Structure and Tautomerism Study of the Mono-protonated Metformin Salt

Xiaodan Wei,<sup>†</sup> Yuhua Fan,<sup>†,\*</sup> Caifeng Bi,<sup>†,\*</sup> Xingchen Yan,<sup>†,‡</sup> Xia Zhang,<sup>†</sup> and Xin Li<sup>†</sup>

<sup>†</sup>Key Laboratory of Marine Chemistry Theory and Technology, Ministry of Education, College of Chemistry and Chemical Engineering, Ocean University of China, Qingdao, Shandong 266100, P.R. China

\*E-mail: fanyuhua301@163.com (Y. Fan); bicai Feng301@163.com (C. Bi)

<sup>‡</sup>Qingdao Institute of Bioenergy and Bioprocess Technology, Chinese Academy of Sciences, Qingdao 266101, P.R. China

Received May 9, 2014, Accepted August 10, 2014

A novel crystal, the mono-protonated metformin acetate (**1**), was obtained and characterized by elemental analysis, IR spectroscopy and X-ray crystallography. It was found that one of the imino group in the metformin cation was protonated along with the proton transfer from the secondary amino group to the other imino group. Its crystal structure was then compared with the previously reported diprotonated metformin oxalate (**2**). The difference between them is that the mono-protonated metformin cations can be linked by hydrogen bonding to form dimers while the diprotonated metformin cations cannot. Both of them are stabilized by intermolecular hydrogen bonds to assemble a 3-D supermolecular structure. The four potential tautomer of the mono-protonated metformin cation (tautomers **1a**, **1b**, **1c** and **1d**) were optimized and their single point energies were calculated by Density Functional Theory (DFT) B3LYP method based on the Polarized Continuum Model (PCM) in water, which shows that the most likely existed tautomer in human cells is the same in the crystal structure. Based on the optimized structure, their Wiberg bond orders, Natural Population Analysis (NPA) atomic charges, molecular electrostatic potential (MEP) maps were calculated to analyze their electronic structures, which were then compared with the corresponding values of the diprotonated metformin cation (cation **2**) and the neutral metformin (compound **3**). Finally, the possible tautomeric mechanism of the mono-protonated metformin cation was discussed based on the observed phenomena.

**Key Words** : Metformin, Crystal structure, Theoretical calculation, Tautomerism

### Introduction

Biguanides are an important class of compounds that have extensive medical applications. As an *N*-substituted derivative of biguanide, metformin (*N,N*-dimethyl biguanide) is a powerful oral antihyperglycemic drug that has been used in many countries for over 40 years for treating diabetic patients with non-insulin-dependent diabetes mellitus.<sup>1</sup> Apart from the well-established antidiabetic and antimalarial effects, biguanide derivatives have been shown to exhibit antimicrobial,<sup>2</sup> antiviral<sup>3</sup> and antiplaque<sup>4</sup> effects and also have been known to influence gastric acid secretion.<sup>5</sup> However, the molecular mechanism for the therapeutic action of these systems is poorly understood. So far, there is much interests in the complexes derived from biguanides with particular attention focused on structural studies,<sup>6</sup> which are beneficial to exploring the relationships between the structure and property.

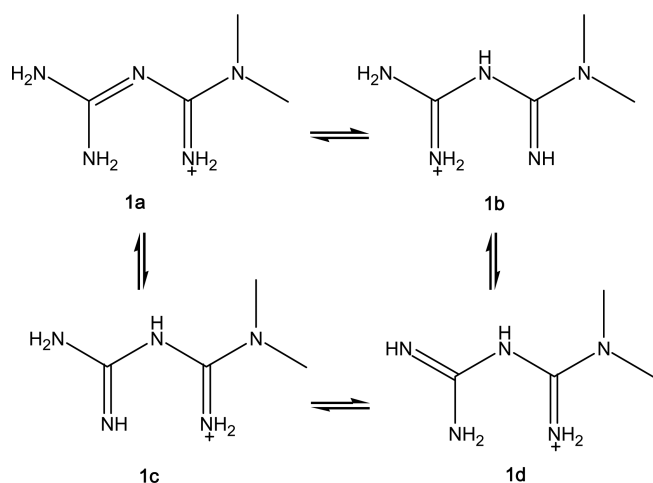
Supermolecular chemistry refers to the assembly of at least two molecules through spontaneous secondary interactions such as hydrogen bonding, dipole-dipole, charge transfer, van der Waals, and  $\pi$ - $\pi$  stacking interactions.<sup>7</sup> This so-called "bottom up" approach to construct nanostructures is advantageous over the "top down" approach such as microlithography which requires substantial effort to fabricate microstructures and devices as the target structures are extended to the range below 100 nm.<sup>8</sup> In addition, essential

biological processes, such as signal transduction, biocatalysis, information storage, and processing, are all based on the supermolecular interactions between molecular components.<sup>9</sup>

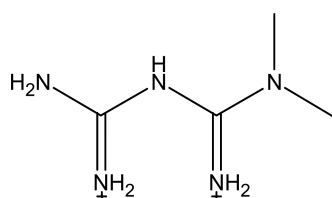
Tautomers are constitutional isomers of organic compounds that readily interconvert by a chemical reaction called tautomerization. This reaction commonly results in the formal migration of a hydrogen atom or proton, accompanied by a switch of a single bond and adjacent double bond. Because of the rapid interconversion, tautomers are generally considered to be the same chemical compound. The different tautomers can potentially exist in each DNA base may play a role in DNA mutation.<sup>10</sup> In addition, tautomerism in bioactive compounds play a key role in orientation of bioactivity of drugs that have found wide application in drug design, from new medicinal materials to antibacterial imidazo[1,2-*a*]pyrimidine (-pyridine),<sup>11</sup> as sulphonamides in the antifungal agents<sup>12</sup> and as potential anti HIV spiro heterocycles.<sup>13</sup>

The crystal structure of diprotonated metformin oxalate has been previously reported.<sup>1</sup> Herein, we report the single crystal of mono-protonated metformin acetate, and compare their crystal structures.

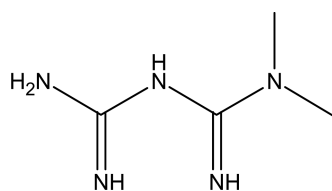
In the crystal structure, it was found that one of the imino group in the metformin cation was protonated along with the proton transfer from the secondary amino group to the other imino group. In view of the observed tautomerism, we speculate that the mono-protonated metformin cation should have four potential tautomers (Scheme 1) in water, although



Scheme 1



Scheme 2



Scheme 3

it exists as tautomer **1a** in the solid state.<sup>14</sup> To well understand its antidiabetic mechanism, raveling which tautomer that actually exists in the body fluid environment is indispensable. As a result, the four potential tautomers of the mono-protonated metformin cation were optimized and their single point energies were calculated by Density Functional Theory (DFT) B3LYP method based on the Polarized Continuum Model (PCM) in water to identify the most likely existed tautomer in human cells. Based on the optimized structure of the most stable tautomer, the Wiberg bond orders, Natural Population Analysis (NPA) atomic charges, molecular electrostatic potential (MEP) maps were calculated to analyze their electronic structures, which were then compared with the corresponding values of the diprotonated metformin cation (Scheme 2) and the neutral metformin (Scheme 3). In addition, as there exist dimers in the crystal structure of tautomer **1a**, we speculate that tautomerism between **1a** and **1d** could proceed through the proton transfer along the hydrogen bonding to each other.

## Experimental

**Materials and Physical Measurements.** All reagents

were of analytical grade and were used as obtained by commercial sources without further purification. Infrared spectra of the compounds were recorded in KBr pellets using a Nicolet 170SX spectrophotometer in the 4000–400  $\text{cm}^{-1}$  region. Elemental analyses were carried out with a model 2400 Perkin-Elmer analyzer. X-ray diffraction data were collected on a Bruker Smart CCD X-ray single-crystal diffractometer.

**Synthesis of Compound 1.** A mixture containing metformin hydrochloride (0.165 g, 1 mmol), KOH (0.056 g, 1 mmol), 2-acetylpyridine (0.121 g, 1 mmol), methanol (20 mL) and ethanol (10 mL) was stirred for 5 h at 55 °C. The obtained solution was filtered and  $\text{Cd}(\text{CH}_3\text{COO})_2 \cdot 2\text{H}_2\text{O}$  (0.266 g, 1 mmol) was added to the filtrate, which was further stirred for 5 h at 55 °C. The resulting solution was filtered and the filtrate was left at room temperature for slow evaporation in air. Colorless block crystals of compound **1** formed after approximately 30 days. mp 248–254 °C Anal. Calcd. (%) for  $\text{C}_6\text{H}_{15}\text{N}_5\text{O}_2$ : C, 38.10; H, 7.94; N, 37.04; O, 16.93. Found (%): C, 38.12; H, 7.93; N, 37.05; O, 16.90. IR (KBr): 3311 s, 3103 s, 1672 s, 1566 s, 1487 s, 1421 sh, 1405 s, 1334 sh, 1281 sh, 1170 w, 1128 w, 1054 m, 1019 sh, 934

**Table 1.** The crystallographic data and structure refinement for compound **1**

Empirical formula	$\text{C}_6\text{H}_{15}\text{N}_5\text{O}_2$
Formula weight	189.23
Temperature (K)	298 (2)
Wavelength (Å)	0.71073
Crystal system	Monoclinic
Space group	$P2(1)/n$
$a$ (Å)	10.0005 (8)
$b$ (Å)	8.9060 (6)
$c$ (Å)	10.7034 (9)
$\alpha$ (°)	90
$\beta$ (°)	91.3130 (10)
$\gamma$ (°)	90
Volume (Å <sup>3</sup> )	953.04 (13)
$Z$	4
Calculated density ( $\text{g}\cdot\text{cm}^{-3}$ )	1.319
Absorption coefficient ( $\text{mm}^{-1}$ )	0.101
$F(000)$	408
Crystal size (mm)	0.45 × 0.40 × 0.24
$\theta$ range for data collection (°)	2.98 to 25.02
Limiting indices	$-11 \leq h \leq 11$ $-10 \leq k \leq 10$ $-12 \leq l \leq 11$
Reflections collected / unique	4619 / 1677 [ $R_{\text{int}} = 0.0239$ ]
Completeness to $\theta = 25.02$	0.996
Max. and min. transmission	0.9761 and 0.9558
Data / restraints / parameters	1677 / 0 / 122
Goodness of fit on $F^2$	1.010
$R_1^a, wR_2^b$ [ $I > 2\sigma(I)$ ]	$R_1 = 0.0426, wR_2 = 0.1099$
$R_1^a, wR_2^b$ (all data)	$R_1 = 0.0557, wR_2 = 0.1225$
Largest diff. peak and hole ( $\text{e}\cdot\text{Å}^{-3}$ )	0.227 and $-0.233$

$$^a R = \sum(|F_o| - |F_c|) / \sum|F_o|. \quad ^b wR = [\sum w(|F_o|^2 - |F_c|^2)^2 / \sum w(F_o^2)]^{1/2}$$

m, 820 m, 761 sh, 728 sh, 653 m, 603 sh.

**Crystallographic Data Collection and Structure Determination.** Diffraction intensity data of the single crystal of compound **1** was collected on a Bruker Smart CCD X-ray single-crystal diffractometer equipped with a graphite monochromated MoK $\alpha$  radiation ( $\lambda = 0.71073 \text{ \AA}$ ) by using a  $\varphi$  and  $\omega$  scan mode at 298 (2) K. The programs used for data collection and cell refinement are the *SMART* and *SAINTE* programs.<sup>15</sup> Empirical absorption correction was applied using the *SADABS* programs,<sup>16</sup> All structure solutions were performed with direct methods using *SHELXS-97*, and the structure refinement was done against  $F^2$  using *SHELXL-97*,<sup>17</sup> All non-hydrogen atoms were found in the final difference Fourier map. All H atoms except for those of the methyl group were found from difference Fourier maps and refined without constraints. The methyl H atoms were positioned geometrically and refined using a riding model, with C–H = 0.96  $\text{\AA}$  and  $U_{\text{iso}}(\text{H}) = 1.5 U_{\text{eq}}(\text{C})$ . Positional and thermal parameters were refined by full-matrix least-squares method to convergence. The molecular graphics were generated using *DIAMOND 3.1D*.<sup>18</sup> The crystallographic data of compound **1** is summarized in Table 1.

**Computational Details.** Optimizations of geometrical structures and Natural Bond Orbital (NBO) analyses of the compounds were carried out by DFT B3LYP method with 6-311+G\* basis set combined with the polarizable continuum model (PCM) in water. The harmonic vibrational frequencies were calculated at the same level of theory for the optimized structure. The vibrational frequency calculations revealed no imaginary frequencies, indicating that a stationary point at this level of approximation was found for the compounds. All calculations were conducted on a Pentium IV computer

using Gaussian 03 program.<sup>19</sup>

Comparison of the optimized bond lengths and angles with the experimental values for tautomer **1a** and cation **2** are available in the supplementary materials. Crystallographic data for compound **1** have been deposited with CCDC (Deposition No. CCDC-991330). These data can be obtained free of charge *via* <http://www.ccdc.cam.ac.uk/conts/retrieving.html> or from CCDC, 12 Union Road, Cambridge CB2 1EZ, UK, E-mail: [deposit@ccdc.cam.ac.uk](mailto:deposit@ccdc.cam.ac.uk).

## Results and Discussion

**Description of the Crystal Structure.** Selected bond lengths and angles of compound **1** are listed in Table 2. The hydrogen bonding geometry for compound **1** is listed in Table 3. As shown in Figure 1(a), the crystal structure of compound **1** is comprised of discrete mono-protonated metformin cations and acetate anions. The cations related by an inversion center are linked *via* N–H $\cdots$ N hydrogen bonds involving the amino groups to form dimers (Figure 1(b)). There are no interactions between each dimers, which are linked by the N–H $\cdots$ O hydrogen bonding between the dimers and the acetate groups to generate an infinite 2-D network (Figure 1(c)). The 2-D network is further connected by N–H $\cdots$ O intermolecular hydrogen bonds to form a 3-D supermolecular structure (Figure 1(d)).

The crystal structure of compound **2** has been reported previously.<sup>1</sup> Compared with compound **1**, N1 cannot serve as the proton receptor to form the dimer as it is protonated. There exist hydrogen bonds between the diprotonated metformin cations and the oxalate anions, giving rise to an infinite 2-D network. These layers are further connected

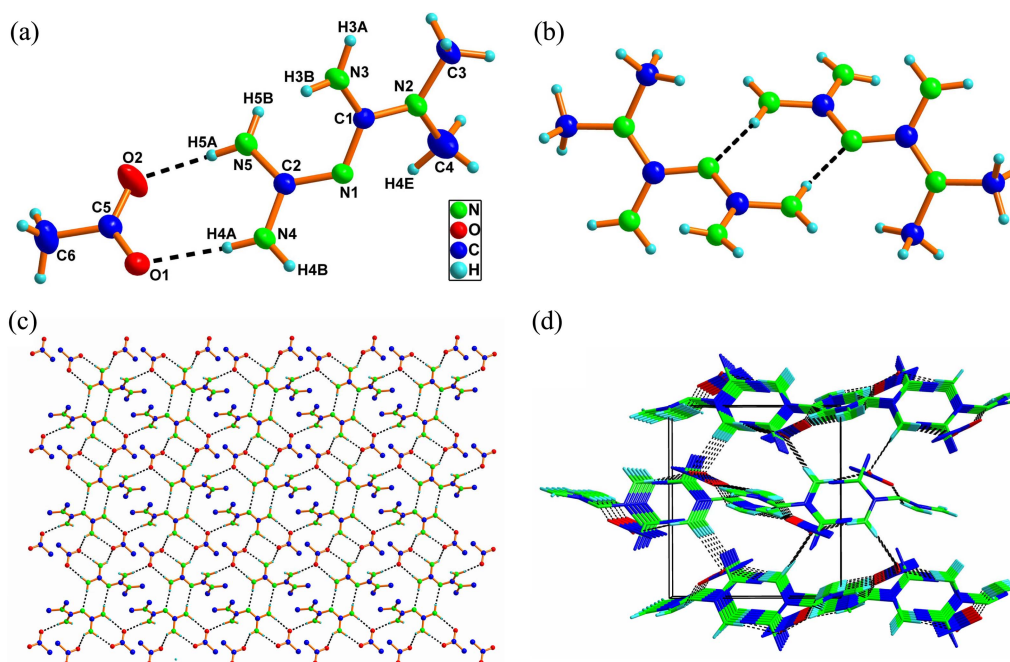


**Figure 1.** (a) The atomic labeling scheme for an asymmetric unit of compound **1**; (b) The dimer connected by hydrogen bonding in compound **1**; (c) The 2-D network in compound **1**; (d) The 3-D supermolecular structure of compound **1**. All hydrogen atoms are omitted for clarity, except for those engaged in hydrogen bonding.

**Table 2.** Selected bond lengths (Å) and angles (°) for compound **1**

Bond	length	Bond	length
N1–C2	1.339(2)	N3–H3A	0.92(3)
N1–C1	1.347(2)	N4–C2	1.332(3)
N2–C1	1.337(2)	N4–H4A	0.87(2)
N2–C4	1.451(3)	N4–H4B	0.88(3)
N2–C3	1.455(3)	N5–C2	1.327(3)
N3–C1	1.333(3)	N5–H5B	0.84(3)
N3–H3B	0.88(3)	N5–H5A	0.84(3)
Bond	Angle	Bond	Angle
C2–N1–C1	121.84(16)	C2–N5–H5B	120.3(16)
C1–N2–C4	121.00(18)	C2–N5–H5A	119.2(17)
C1–N2–C3	122.73(17)	H5B–N5–H5A	117(2)
C4–N2–C3	116.26(17)	N3–C1–N2	119.33(18)
C1–N3–H3B	116.7(16)	N3–C1–N1	122.27(18)
C1–N3–H3A	124.3(15)	N2–C1–N1	118.19(17)
H3B–N3–H3A	119(2)	N5–C2–N4	117.30(18)
C2–N4–H4A	121.0(15)	N5–C2–N1	124.57(18)
C2–N4–H4B	119.0(16)	N4–C2–N1	118.04(17)
H4A–N3–H4B	120(2)		

**Table 3.** Hydrogen bonding geometry for compound **1** (Å, °)

<i>D</i> –H... <i>A</i>	<i>D</i> –H	H... <i>A</i>	<i>D</i> ... <i>A</i>	<i>D</i> –H... <i>A</i>
N3–H3A...O1 <sup>a</sup>	0.92(3)	2.05(3)	2.960(2)	172(2)
N3–H3B...O1 <sup>b</sup>	0.88(3)	2.18(3)	3.028(2)	163(2)
N4–H4A...O1	0.88(2)	2.08(2)	2.955(2)	173(2)
N4–H4B...N1 <sup>c</sup>	0.88(2)	2.23(2)	3.103(3)	174(2)
N5–H5A...O2 <sup>d</sup>	0.84(2)	1.98(3)	2.814(2)	177(2)
N5–H5B...O2 <sup>d</sup>	0.84(2)	2.11(2)	2.830(3)	143(2)
C4–H4E...N1	0.9600	2.3700	2.734(3)	102.00

Symmetry codes: <sup>a</sup>*x*, *y*+1, *z*; <sup>b</sup>–*x*+1/2, *y*+1/2, –*z*+1/2; <sup>c</sup>–*x*+1, –*y*+1, –*z*+1; <sup>d</sup>–*x*+1, –*y*+1, –*z*.

through N–H...O intermolecular hydrogen bonds to form the 3-D supermolecular structure. But both of them have strong double hydrogen bonds between either the carboxylate

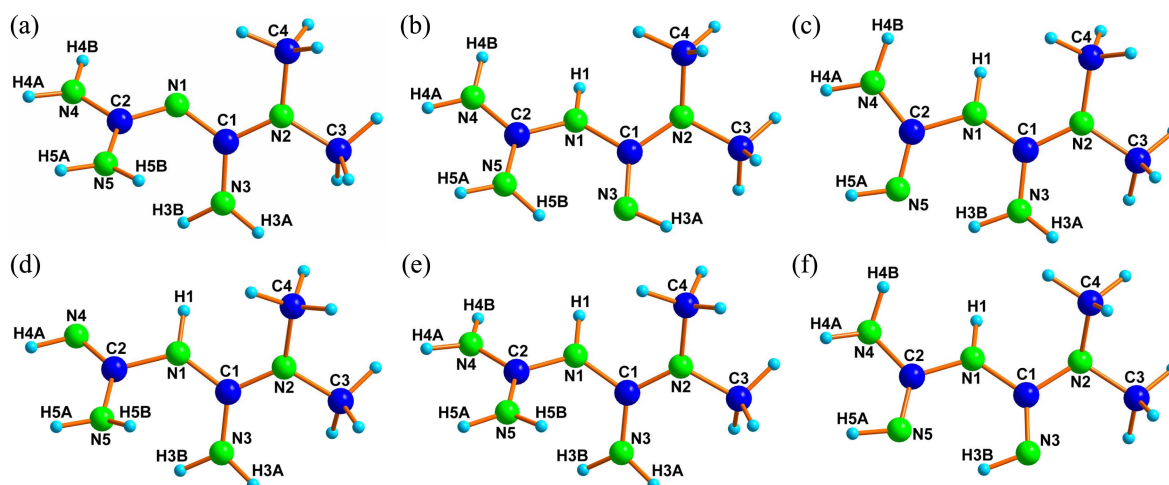
groups of the acetate anion or the oxalate anion and atoms N1 and N4 of the metformin cation.

**Quantum Chemistry Calculations.** The optimized geometries of tautomers **1a**, **1b**, **1c**, **1d**, cation **2** and compound **3** are shown in Figure 2. Comparison of the optimized bond lengths and angles with the experimental values for tautomer **1a** and cation **2** are shown in Tables S1 and S2 in the supplementary material, respectively. The calculated values are consistent to the experimental values, except for the N–H bond lengths. This is because the molecules were calculated in the water environment while the experimental values were measured in the solid state. Water molecules have a large impact on the N–H bond lengths through hydrogen bonding. Comparison of the corresponding Wiberg bond orders for tautomers **1a**, **1b**, **1c**, **1d**, cation **2** and compound **3** is made in Table 4. Comparison of corresponding NPA atomic charges for tautomers **1a**, **1b**, **1c**, **1d**, cation **2** and compound **3** is made in Table 5.

For tautomer **1a**, the Wiberg bond orders of N1–C1, N2–C1, N4–C2, N5–C2, N3–C1 and N1–C2 are almost equal, and they are higher than single bond and lower than double bond (Table 4). This suggests that tautomer **1a** has a large extent of delocalization. The total NPA atomic charge distributed on N3H3AH3B is 0.081 (Table 5). This suggests that the positive charge brought by the N3 protonation has partially transferred to N1, N2, N4, N5, C2 and C1 through

**Table 4.** Comparison of the corresponding Wiberg bond orders for tautomers **1a**, **1b**, **1c**, **1d**, cation **2** and compound **3**

Bond	<b>1a</b>	<b>1b</b>	<b>1c</b>	<b>1d</b>	<b>2</b>	<b>3</b>
N1–C2	1.3187	1.1818	1.0036	0.9909	1.1170	1.0781
N1–C1	1.2850	1.0039	1.1710	1.1767	1.0768	1.0430
N2–C1	1.2577	1.1343	1.2776	1.2957	1.3572	1.0702
N2–C4	0.9399	0.9452	0.9371	0.9360	0.9277	0.9579
N2–C3	0.9488	0.9558	0.9381	0.9382	0.9308	0.9598
N3–C1	1.2622	1.7091	1.3510	1.3233	1.3614	1.7449
N4–C2	1.2886	1.3210	1.2163	1.7437	1.3823	1.1468
N5–C2	1.2622	1.3604	1.6761	1.1713	1.3679	1.6736

**Figure 2.** The optimized geometry of (a) tautomer **1a**; (b) tautomer **1b**; (c) tautomer **1c**; (d) tautomer **1d**; (e) cation **2**; (f) compound **3**.

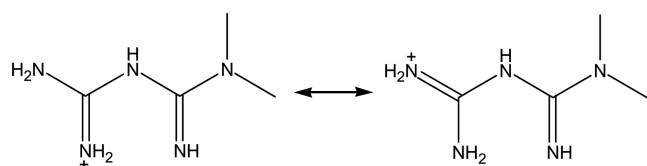
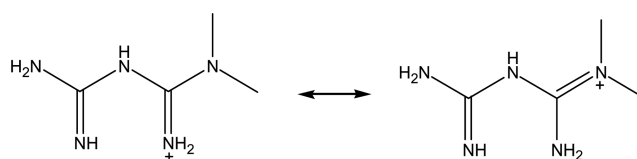
**Table 5.** Comparison of the corresponding NPA atomic charges for tautomers **1a**, **1b**, **1c**, **1d**, cation **2** and compound **3**

Atom	<b>1a</b>	<b>1b</b>	<b>1c</b>	<b>1d</b>	<b>2</b>	<b>3</b>
N1	-0.674	-0.624	-0.579	-0.480	-0.611	-0.585
H1		0.492	0.469	0.485	0.527	0.439
N2	-0.456	0.139	0.178	0.176	0.204	0.183
N3	-0.778	-0.706	-0.788	-0.732	-0.715	-0.659
H3A	0.426	0.379	0.442	0.461	0.480	
H3B	0.433		0.522	0.464	0.483	0.377
N4	-0.760	-0.811	-0.750	-0.643	-0.754	-0.664
H4A	0.428	0.491	0.447	0.363	0.505	0.395
H4B	0.433	0.458	0.430		0.468	0.390
N5	-0.785	-0.863	-0.836	-0.754	-0.805	-0.769
H5A	0.430	0.498	0.419	0.442	0.518	0.373
H5B	0.430	0.483		0.418	0.481	
C1	0.679	0.189	0.425	0.350	0.377	0.027
C2	0.652	0.804	0.511	0.328	0.676	0.372
C3	-0.368	-0.752	-0.811	-0.799	-0.808	-0.627
C4	-0.348	-0.799	-0.807	-0.821	-0.829	-0.763

conjugation. The dihedral angle between plane 1 formed by N4–C2–N1–N5 and plane 2 formed by N1–C1–N2–N3 is 51.41°, indicating that N5–C2 and N3–C1 are not coplanar. This is result from the steric hindrance between H3B and H5B.

For tautomer **1b**, the Wiberg bond orders of N3–C1 is close to that of double bond. The Wiberg bond orders of N1–C2, N1–C1 and N2–C1 are close to that of single bond. Furthermore, the Wiberg bond orders of N4–C2 and N5–C2 are almost equal, and they are higher than single bond and lower than double bond. This suggests that the structure of tautomer **1b** can be described as the resonance between the two structures shown in Scheme 4. The total NPA atomic charge distributed on N5H5AH5B (0.118) and N4H4AH4B (0.138) are almost equal, because the positive charge brought by the N5 protonation has partially transferred to N4 through resonance. The dihedral angle (19.30°) between plane 1, N4–C2–N1–N5 and plane 2, N1–C1–N2–N3 is smaller than the corresponding dihedral angle in tautomer **1a**. This is because only H3A is connected with N3, and thereby the intramolecular hydrogen bond N5–H5B...N3 was formed to eliminate the steric hindrance.

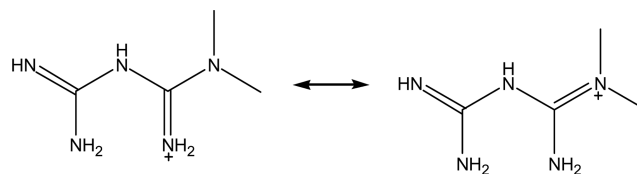
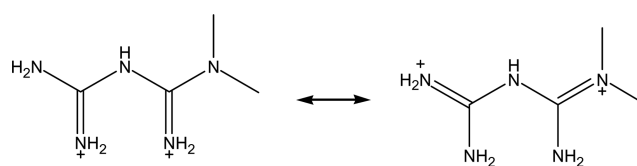
For tautomer **1c**, the Wiberg bond order of N5–C2 is close to that of double bond. The Wiberg bond orders of N1–C2, N4–C2 and N1–C1 are close to that of single bond. Furthermore, the Wiberg bond orders of N3–C1 and N2–C1 are almost equal, and they are higher than single bond and lower than double bond. This suggests that tautomer **1c** can be described as the resonance between the two structures in

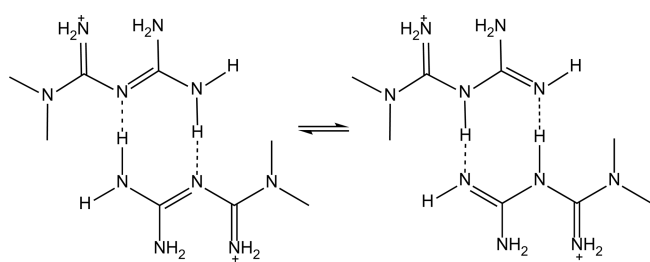
**Scheme 4****Scheme 5**

Scheme 5. The total NPA atomic charge distributed on N3H3AH3B is 0.176, which indicate that the positive charge brought by the N3 protonation has partially transferred to N2 through resonance. The dihedral angle (11.06°) of plane 1, N4–C2–N1–N5 and plane 2, N1–C1–N2–N3 is also smaller than the corresponding dihedral angle of tautomer **1a**. This is due to the formation of intramolecular hydrogen bond N3–H3B...N5.

For tautomer **1d**, the Wiberg bond order of N4–C2 is close to that of double bond. The Wiberg bond orders of N5–C2, N1–C2 and N1–C1 are close to that of single bond. Furthermore, the Wiberg bond orders of N3–C1 and N2–C1 are almost equal, and they are higher than single bond and lower than double bond. This suggests that tautomer **1d** can be described as the resonance between the two structures shown in Scheme 6. The total NPA atomic charge distributed on N3H3AH3B is 0.193, indicating that the positive charge brought by the N3 protonation has partially transferred to N2 through resonance. The dihedral angle (46.14°) of plane 1, N4–C2–N1–N5 and plane 2, N1–C1–N2–N3 is similar to the corresponding dihedral angle of tautomer **1a**. This is also attributed to the steric hindrance between H3B and H5B. For compound **1**, the delocalization extent of tautomer **1a** is the largest, indicating that it is the most stable structure in aqueous environment.

For cation **2**, the Wiberg bond orders of N1–C2 and N1–C1 are close to that of single bonds. Furthermore, the Wiberg bond orders of N4–C2, N5–C2, N2–C1 and N3–C1 are almost equal, and they are higher than single bond and lower than double bond. This suggests that cation **2** can be described as the resonance between the two structures shown in Scheme 7. The total NPA atomic charge distributed on N5H5AH5B (0.194), N4H4AH4B (0.219) and N3H3AH3B

**Scheme 6****Scheme 7**



Scheme 8

(0.248) are almost equal, because the positive charge brought by the N3 and N5 protonation has partially transferred to N2 and N4 through resonance, respectively. The dihedral angle ( $56.36^\circ$ ) of plane 1, N4–C2–N1–N5 and plane 2, N1–C1–N2–N3 is larger than the corresponding dihedral angle in tautomer **1a**. The steric hindrance between H3B and H5B is larger because there is more positive charge on N3 and N5, which increases the repulsive force between H3B and H5B.

For compound **3**, the Wiberg bond order of N5–C2 and N3–C1 are close to that of double bond. The Wiberg bond orders of N4–C2, N1–C2, N2–C1 and N1–C1 are close to that of single bond. This suggests that the delocalization extent of compound **3** is very small. The dihedral angle ( $9.76^\circ$ ) between plane 1, N4–C2–N1–N5 and plane 2, N1–C1–N2–N3 is similar to the corresponding dihedral angle of tautomer **1c**. This is also ascribed to the intramolecular hydrogen bond N3–H3B $\cdots$ N5, which eliminates the steric hindrance.

The calculated molecular total energies of tautomers **1a** (–433.423 a.u.), **1b** (–433.410 a.u.), **1c** (–433.407 a.u.) and **1d** (–433.403 a.u.) suggest that the total molecular energy of tautomer **1a** is the lowest. This is consistent to the previous conclusion that tautomer **1a** is the most stable structure in aqueous solution.

Since there exist dimers in the crystal structure of compound **1**, we speculate that the dimers also exist in aqueous solution. As a result, the tautomerism between **1a** and **1d** can proceed through the proton transfer along the hydrogen bond to each other, as shown in Scheme 8. In addition, as tautomer **1b** and **1c** could form intramolecular hydrogen bond N5–H5B $\cdots$ N3 and N3–H3B $\cdots$ N5, the tautomerism between **1b** and **1c** is most likely to proceed through the proton transfer between N3 and N5 along the hydrogen bond.

### Conclusion

The single crystal of mono-protonated metformin acetate was obtained and characterized by elemental analysis, IR spectroscopy and X-ray crystallography. One of the imino groups in the metformin cation was protonated along with the proton transfer from the secondary amino group to the other imino group. Its crystal structure was then compared with the previously reported diprotonated metformin oxalate. The difference between them is that the mono-protonated

metformin cations can be linked by hydrogen bonding to form dimers while the diprotonated metformin cations cannot. Both of them are stabilized by intermolecular hydrogen bonds to assemble a 3-D supermolecular structure. Theoretical calculations based on the optimized geometries of tautomers **1a**, **1b**, **1c**, **1d**, cation **2** and compound **3** indicate that the positive charge brought by protonation can partially transfer to the adjacent N atoms along with the resonance and conjugation. Tautomer **1a** has the largest extent of electron delocalization, the most even electrostatic potentials on N atoms and the lowest molecular energies in aqueous environment, which suggests that the mono-protonated metformin cation most likely exist as tautomer **1a** in human cells. In addition, the tautomerism between **1a** and **1d** can proceed through the proton transfer along the hydrogen bond to each other, and the tautomerism between **1b** and **1c** is most likely to proceed through the proton transfer between N3 and N5 along the hydrogen bond.

**Acknowledgments.** This research was supported by the Specialized Research Fund for the Doctoral Program of Higher Education of China (grant No. 20120132110015), the National Natural Science Foundation of China (grant Nos. 21371161, 21071134 and 20971115), the Special Foundation for Young Teachers of Ocean University of China (grant No. 201113025) and the Natural Science Foundation of Shandong Province (grant No. ZR2012BQ026).

### References

- Lu, L. P.; Zhang, H. M.; Feng, S. S.; Zhu, M. L. *Acta Cryst.* **2004**, *C60*, o740.
- Thomas, L.; Russell, A. D.; Maillard, J. Y. *J. Appl. Microbiol.* **2005**, *98*, 533.
- Denys, A.; Machlanski, T.; Bialek, J.; Mrozicki, S. *Praeventivmedizin* **1977**, *164*, 85.
- Tanzer, J. M.; Slee, A. M.; Kamay, B. A. *Antimicrob. Agents Chemother.* **1977**, *12*, 721.
- (a) Pinelli, A.; Trivulzio, S.; Pojaga, G.; Rossoni, G. *Pharmacol. Res.* **1996**, *34*, 225. (b) Pinelli, A.; Colombo, R.; Trivulzio, S.; Berti, F.; Tofanetti, O.; Caimi, B. R. *Arzneim. Forsch.* **1984**, *34*, 890.
- Bailey, P. J.; Pace, S. *Coord. Chem. Rev.* **2001**, *214*, 91.
- (a) Rebek, J., Jr.; *Angew. Chem. Int. Ed.* **1990**, *29*, 245. (b) Amabilino, D. B.; Stoddart, J. F. *Chem. Rev.* **1995**, *95*, 2715. (c) Fyfe, M. C. T.; Stoddart, J. F. *Acc. Chem. Res.* **1997**, *30*, 393. (d) Harada, A.; Li, J.; Kamachi, M. *Nature* **1992**, *356*, 325. (e) Harada, A.; Li, K.; Kamachi, M. *Nature* **1994**, *370*, 126.
- Whitesides, G. M.; Mathias, J. P.; Seto, C. T. *Science* **1991**, *254*, 1312.
- Albrecht, M. *Naturwissenschaften* **2007**, *94*, 951.
- Akai, N.; Ohno, K.; Aida, M. *Chem. Phys. Lett.* **2005**, *413*, 306.
- (a) Mahadevan, S.; Palaniandavar, M. *Inorg. Chem.* **1998**, *37*, 693. (b) Kashanian, S.; Gholivand, M. B.; Ahmadi, F.; Taravati, A.; Hosseinzadeh Colagar, A. *J. Spectrochim. Acta* **2007**, *A67*, 472.
- Carter, M. T.; Rodriguez, M.; Bard, A. J. *J. Am. Chem. Soc.* **1989**, *111*, 8901.
- Liu, C. L.; Zhou, J. Y.; Li, Q. X.; Wang, L. J.; Liao, Z. R.; Xu, H. B. *J. Inorg. Biochem.* **1999**, *75*, 233.
- Bharatam, P. V.; Patel, D. S.; Iqbal, P. J. *Med. Chem.* **2005**, *48*, 7615.
- SMART and SAINT, Area Detector Control and Integration

- Software. Siemens Analytical X-ray Systems, Inc. Madison, WI, 1996.
16. Bruker AXS, SAINT Software Reference Manual. Madison, WI, 1998.
17. Sheldrick, G. M. *Acta Cryst.* **2008**, *A64*, 112.
18. Brandenburg, K. *DIAMOND, version 3.1D*, Crystal Impact GbR, Born, Germany, 2006.
19. Frisch, K. D.; Trucks, G. W.; Schlegel, H. B.; Robb, M. A.; Cheeseman, J. R.; Zakrzewski, V. G.; Montgomery, J. A. *Gaussian 03, Revision A. 6*. Gaussian, Inc. Pittsburgh, Pennsylvania, USA, 2003.
-